Supporting information

Highly Active and Stable Large Mo-doped Pt-Ni Octahedral Catalysts for ORR: Synthesis, Post-treatments and Electrochemical Performance and Stability

Shlomi Polani,[*a†] Katherine E. MacArthur,[b†] Jiaqi Kang,[a] Malte Klingenhof,[a] Xingli Wang,[a]

Tim Möller,[a] Raffaele Amitrano,[a] Raphaël Chattot,[c] Marc Heggen,[*b] Rafal E. Dunin-Borkowski,[b] and Peter Strasser[*a]

[a]Electrochemical Energy, Catalysis and Material Science Laboratory, Department of Chemistry, Technical University Berlin, 10623 Berlin, Germany

[b]Ernst-Ruska Centre for Microscopy and Spectroscopy with Electrons and Peter Grünberg Institute, Forschungszentrum Jülich GmbH, 52425 Jülich, Germany

[c]ICGM, Univ. Montpellier, CNRS, ENSCM, 34095 Montpellier cedex 5, France

†These authors contributed equally to the article.

Corresponding Authors

pstrasser@tu-berlin.de
m.heggen@fz-juelich.de
polani@tu-berlin.de

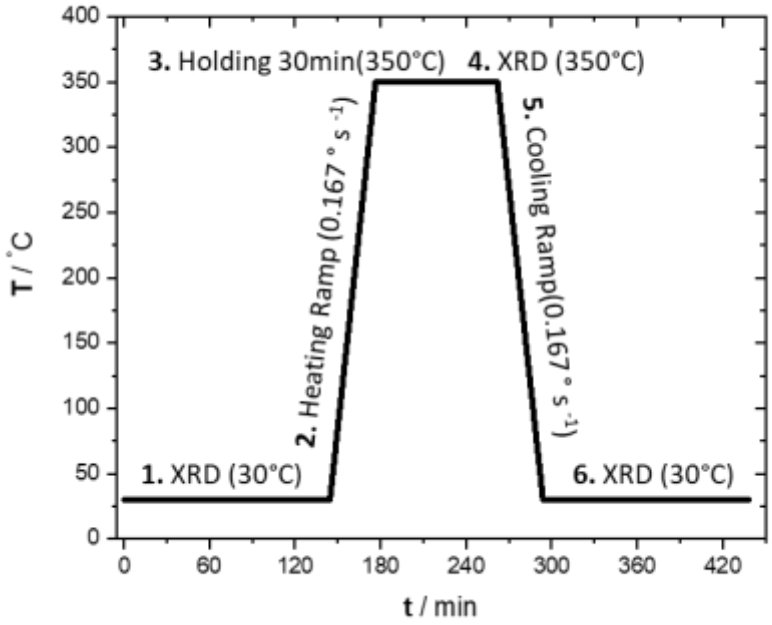

Figure S1. Heating protocol for in situ high-temperature XRD.

Scheme S1. Detailed testing protocols for this study.

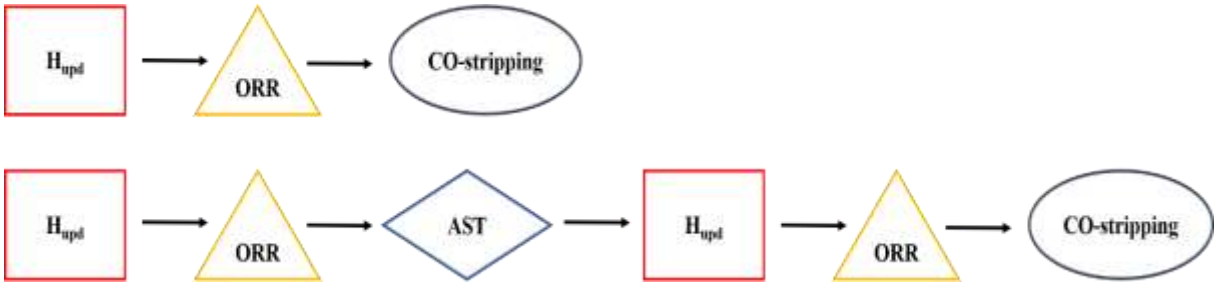

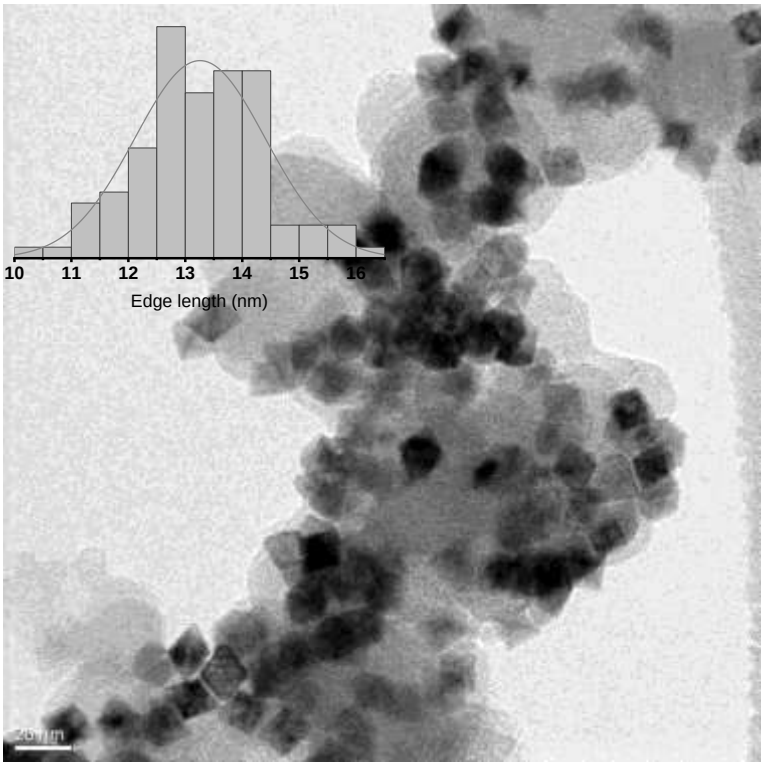

Figure S2. TEM image and the corresponding edge length distribution histogram for PtNi-13 octahedral NPs

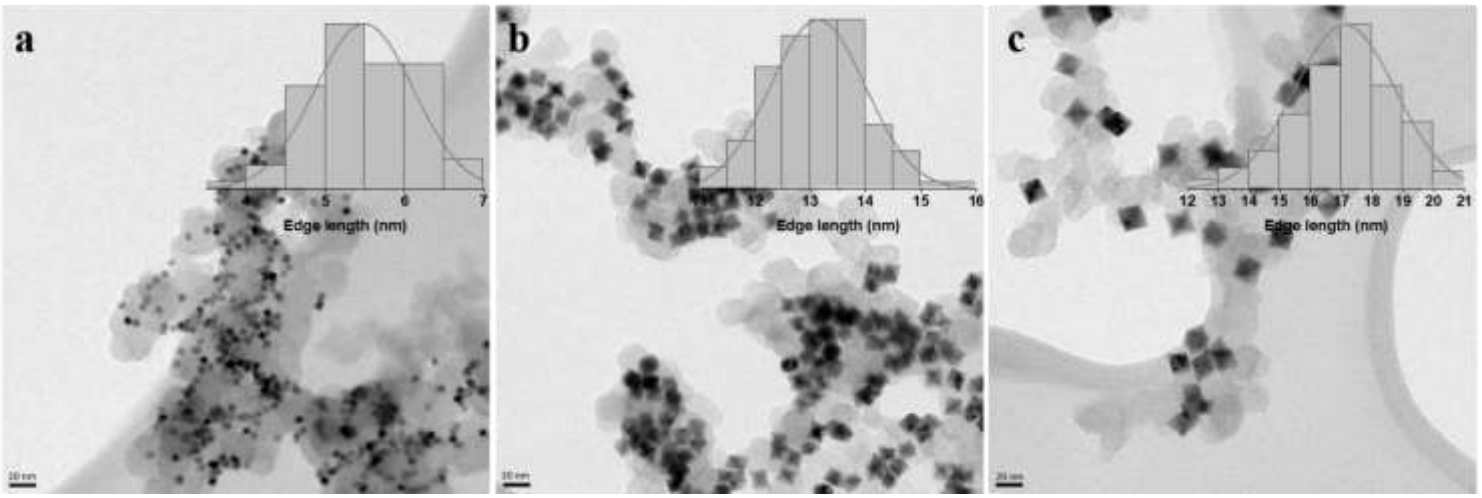

Figure S3. Transmission electron microscopy (TEM) images and the corresponding edge length distribution histogram for PtNi(Mo)/C octahedral NPs (a) PtNi(Mo)-5 (b) PtNi(Mo)-13 (c) PtNi(Mo)-17.

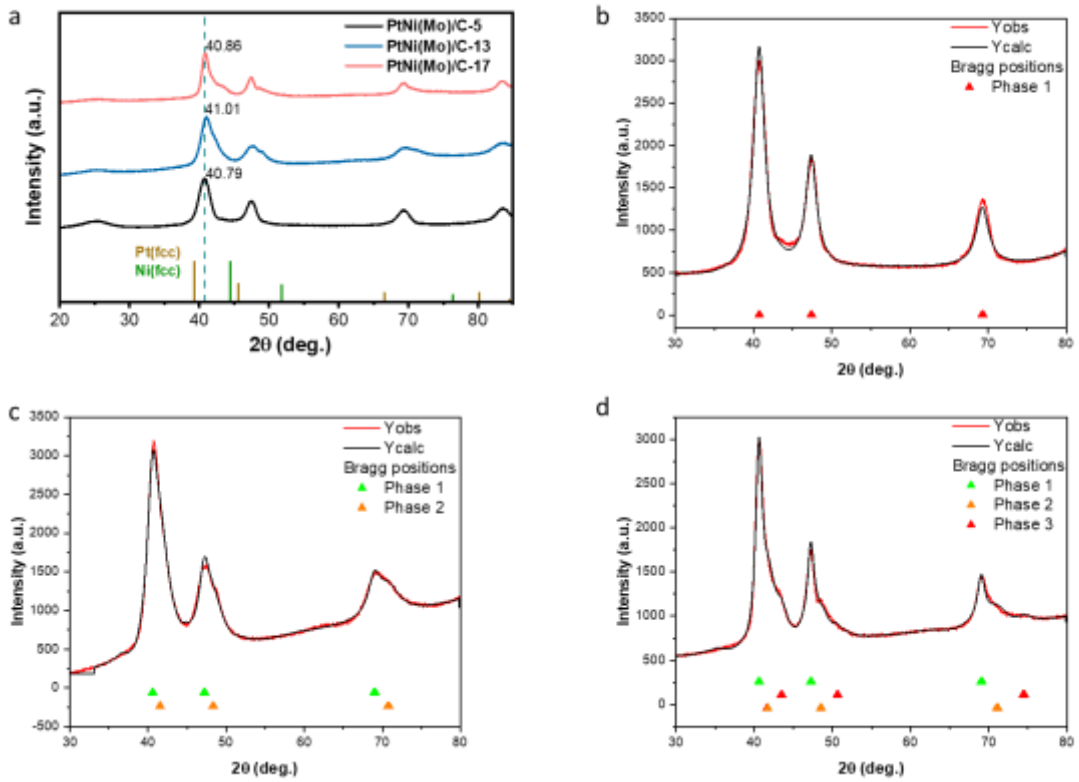

Figure S4. (a) XRD pattern of oh-PtNi(Mo)-5, oh-PtNi(Mo)-13, oh-PtNi(Mo)-17, brown columns correspond to pure Pt (PDF no. 00-004-0802) and green columns to pure Ni (PDF no. 00-004-0850) patterns. The deconvolution of the XRD patterns and the corresponding Bragg positions of the different phases for (b) PtNi(Mo)-5, (c) PtNi(Mo)-13 and (d) PtNi(Mo)-17.

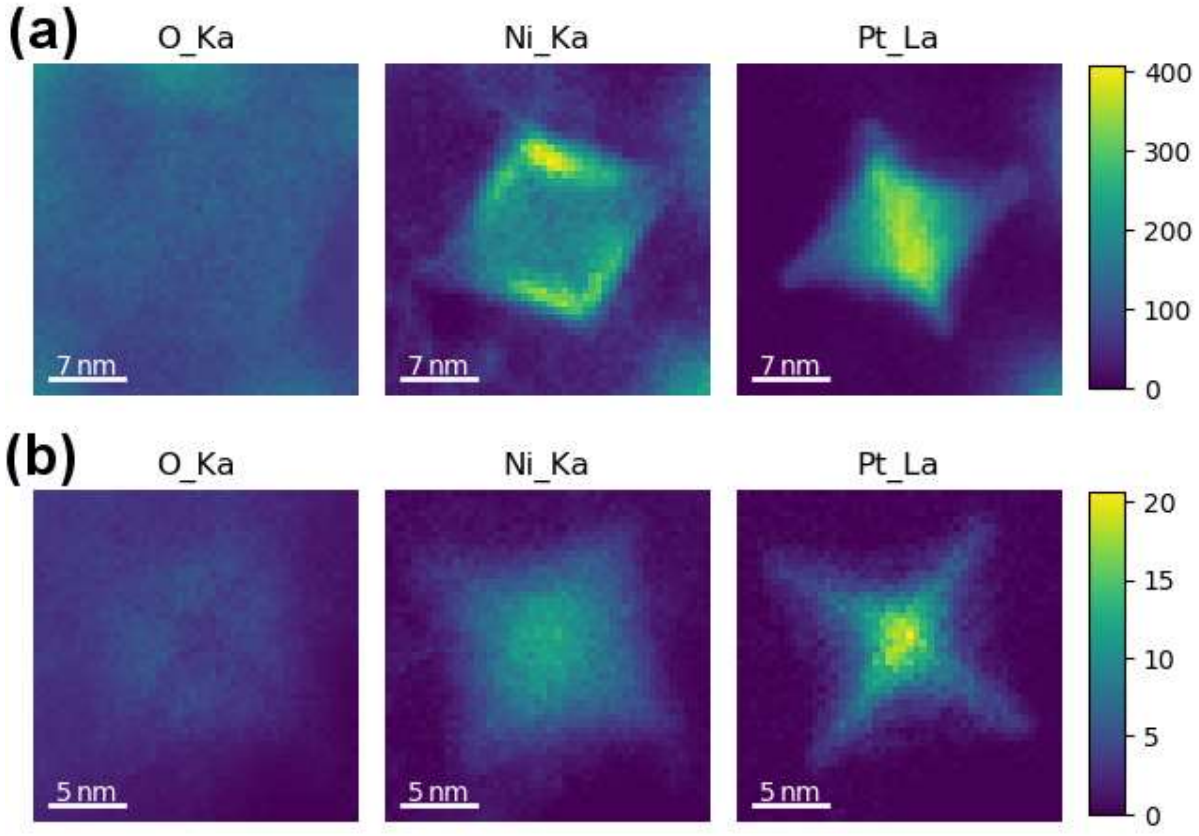

Figure S5. As-prepared oh-PtNi(Mo)-17: EDS Elemental maps, after NMF analysis for O Ka, Ni Ka and Pt La plotted on the same intensity scale viewed (a) along <110> and (b) along <100> directions. The intensity scale is in X-ray counts.

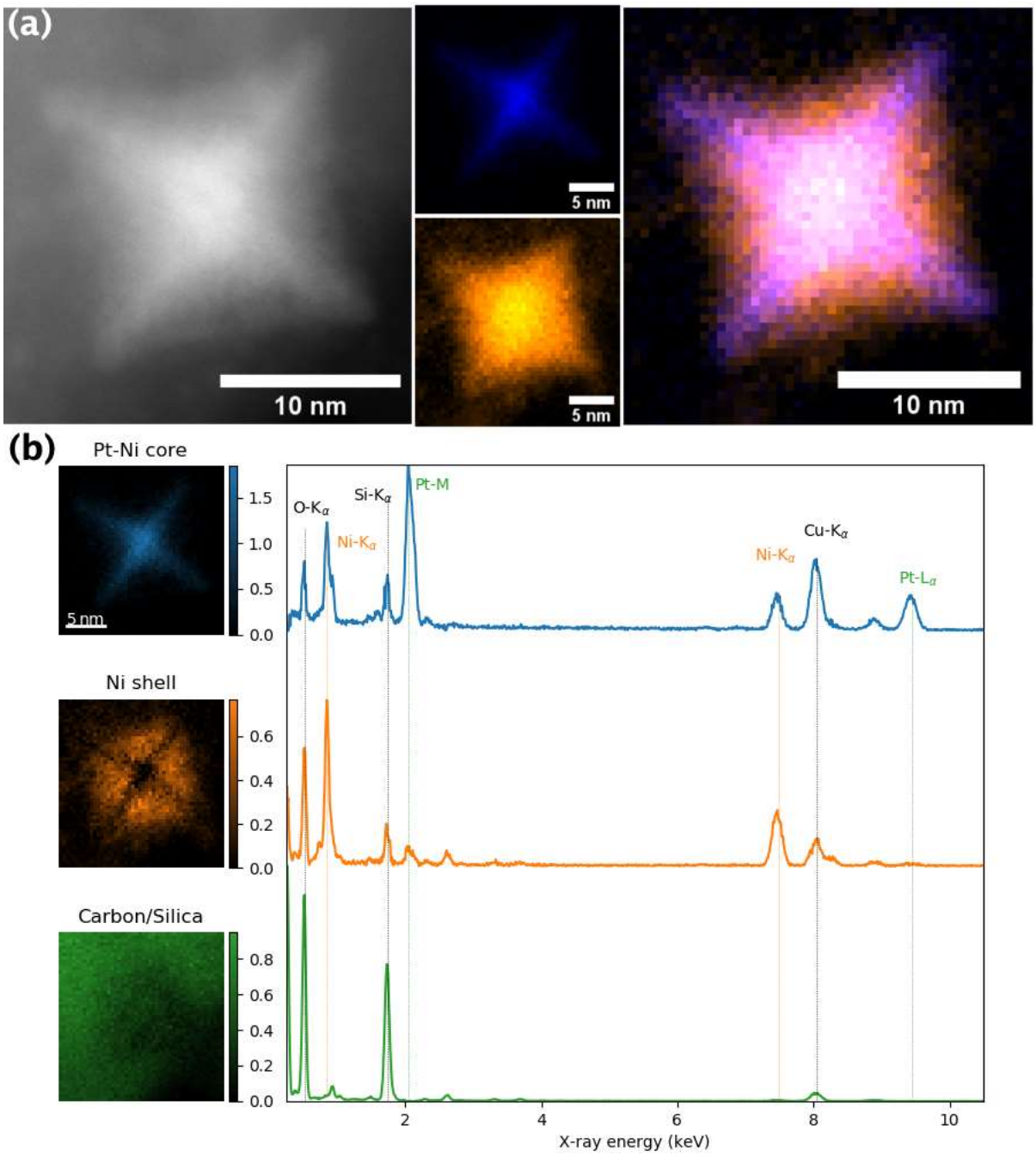

Figure S6. As-prepared oh-PtNi(Mo)-17: (a) ADF-STEM micrographs, STEM-EDS elemental mapping for Pt (blue) and Ni (orange), and their overlay, viewed along a <100> direction. (b) (b) EDS NMF component maps and corresponding spectra show the distribution of a Pt-rich core (blue), a Ni- and O-rich shell (orange), as well as C and Si (green).

Table S1. Metallic at.%, mean edge length, Pt wt% and crystal structure of octahedral PtNi(Mo)/C samples, estimated from ICP-OES, TEM and Rietveld refinement of XRD patterns.

PtNi(Mo)-L	Metallic at% ICP-OES	Mean Edge length (nm)	Pt wt%	Rietveld refinement					
				Phase	Ni at. %	a	wt. %	size [nm]	R_{Bragg} (%)
PtNi(Mo)-5	$Pt_{67.7}Ni_{31}Mo_{1.3}/C$	5.5 ± 0.6	12.6	1	20.843	3.836	100	3.5	1.78
PtNi(Mo)-13	$Pt_{28.2}Ni_{70.8}Mo_{1.0}/C$	13.1 ± 0.9	20.1	1st	17.213	3.851	31.864	3.7	0.54
				2nd	38.338	3.766	68.135	1.9	0.076
PtNi(Mo)-17	$Pt_{32.5}Ni_{67}Mo_{0.5}/C$	17.1 ± 1.6	18.6	1st	18.025	3.847	29.361	6	1.26
				2nd	41.849	3.752	58.255	2.1	0.26
				3rd	78.717	3.605	12.382	3.7	0.32
PtNi(Mo)-17H	$Pt_{31.7}Ni_{67.9}Mo_{0.4}/C$	13.7 ± 1.62	20.4						
PtNi-13	$Pt_{14.7}Ni_{85.3}/C$	13.26 ± 1.15	19.3						

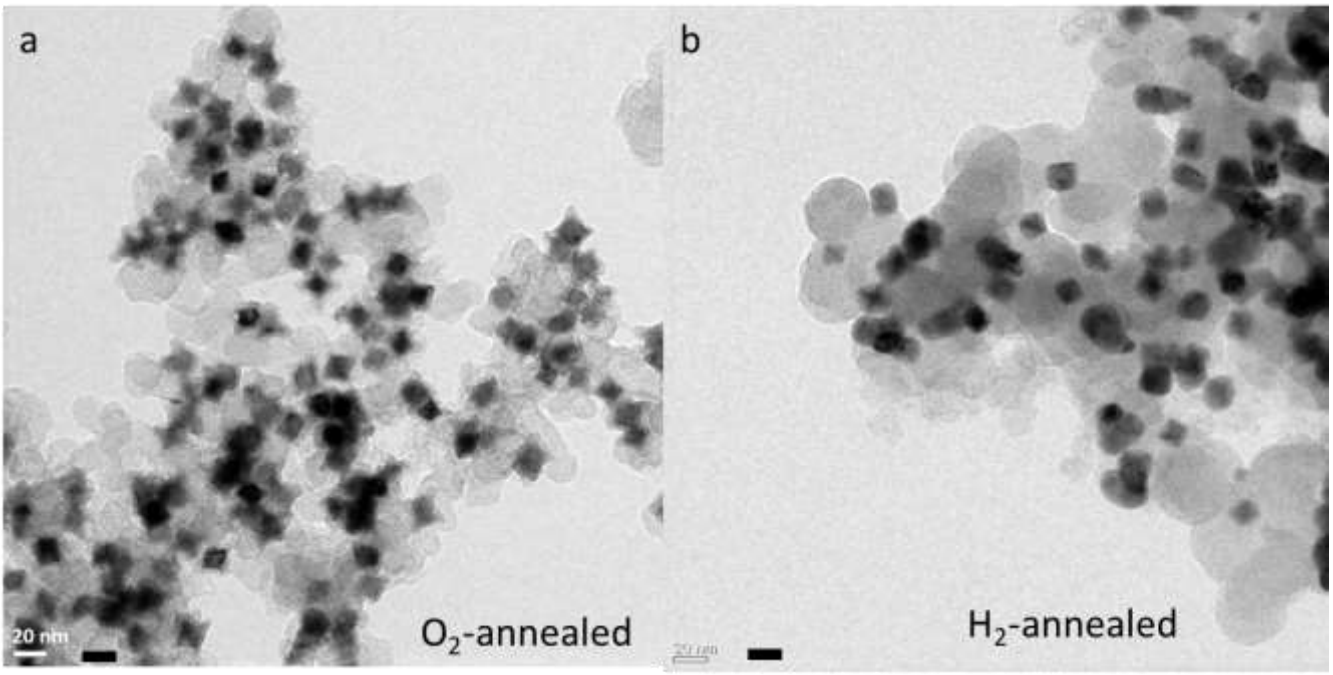

Figure S7. TEM images of oh-PtNi(Mo)-17 after annealing in (a) air or (b) H_2 environment.

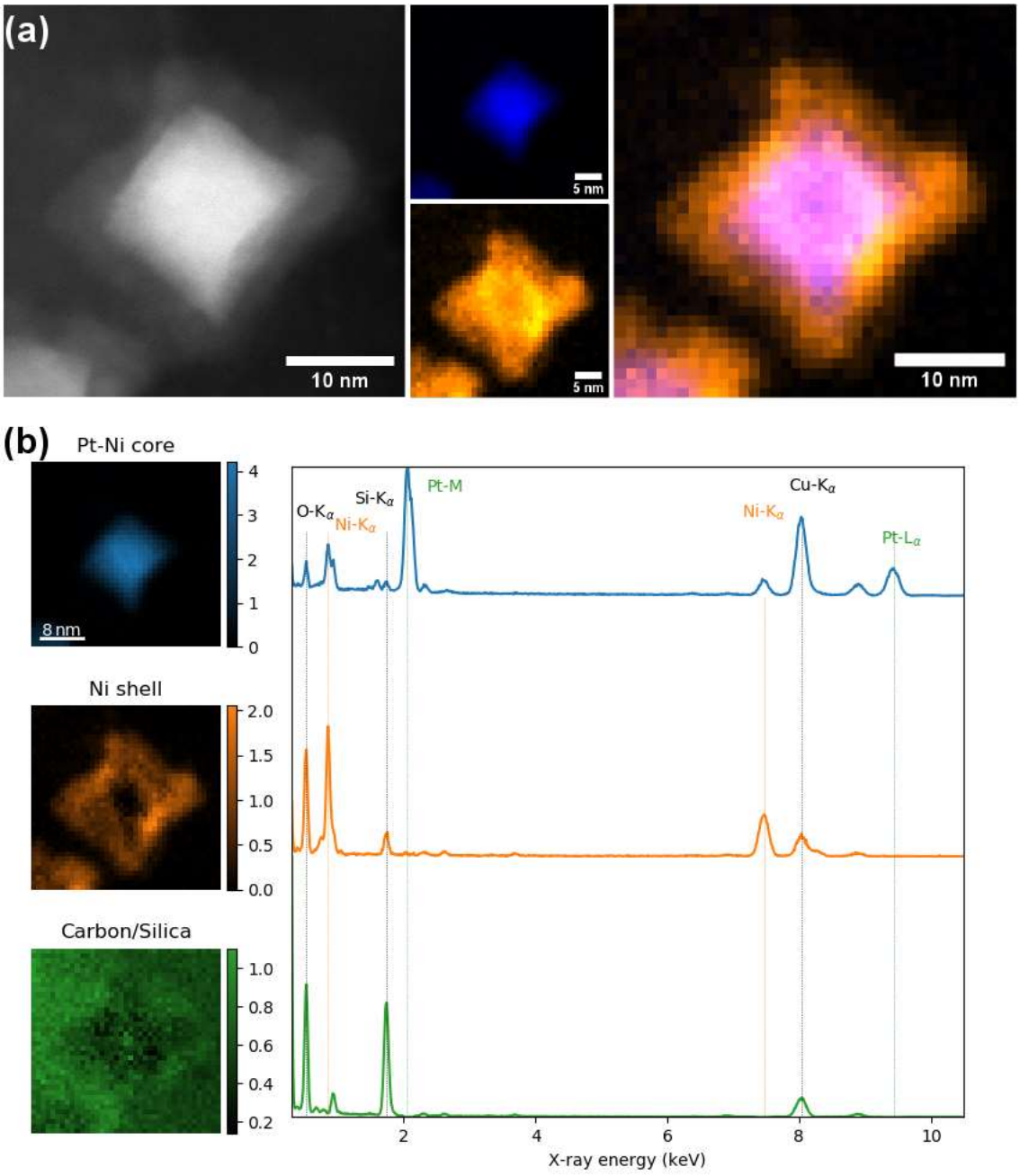

Figure S8. Air-annealed oh-PtNi(Mo)-17A: (a) ADF-STEM micrograph and STEM-EDS elemental mapping for Pt (blue) and Ni (yellow), and their overlay, viewed a) along a <100> direction. (b) EDS NMF component maps and corresponding spectra show the distribution of a Pt-rich core (blue), a Ni- and O-rich shell (orange), as well as C and Si (green).

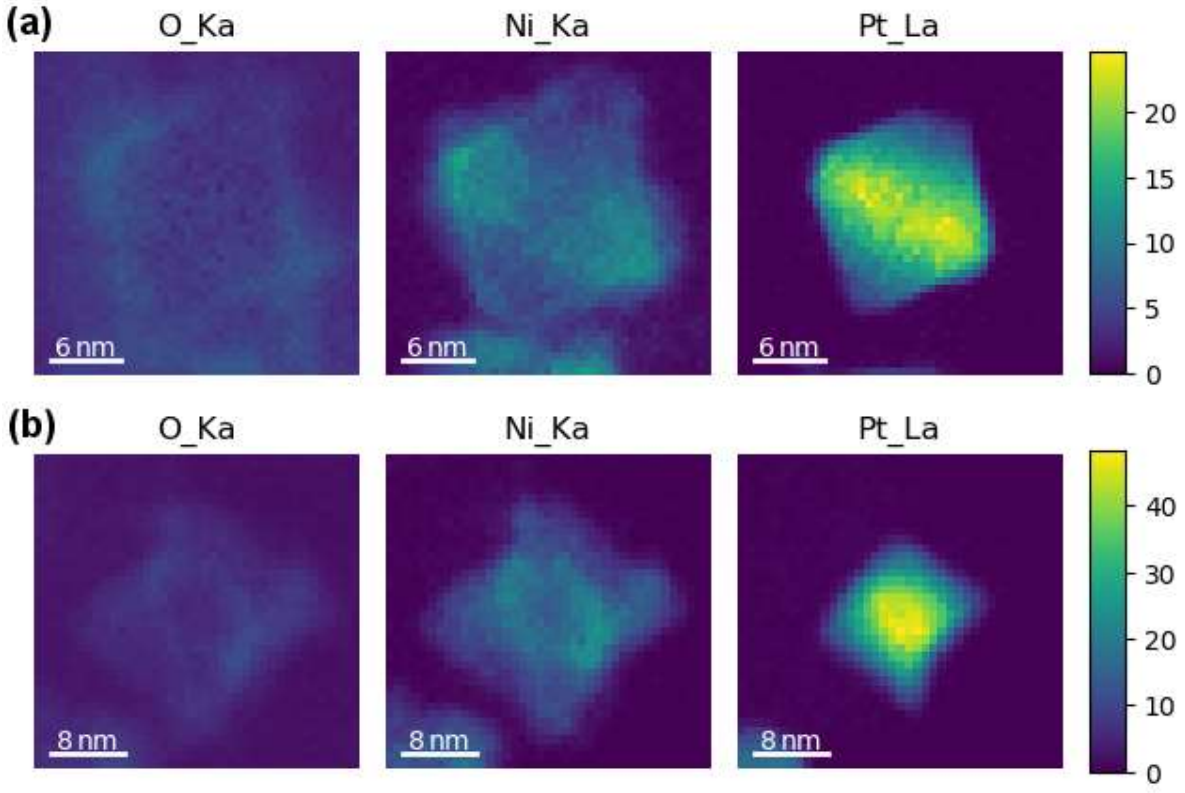

Figure S9. Air-annealed oh-PtNi(Mo)-17A: EDS Elemental maps, after NMF analysis for O Ka, Ni Ka and Pt La plotted on the same intensity scale viewed (a) along <110> and (b) along <100> directions. The intensity scale is in X-ray counts.

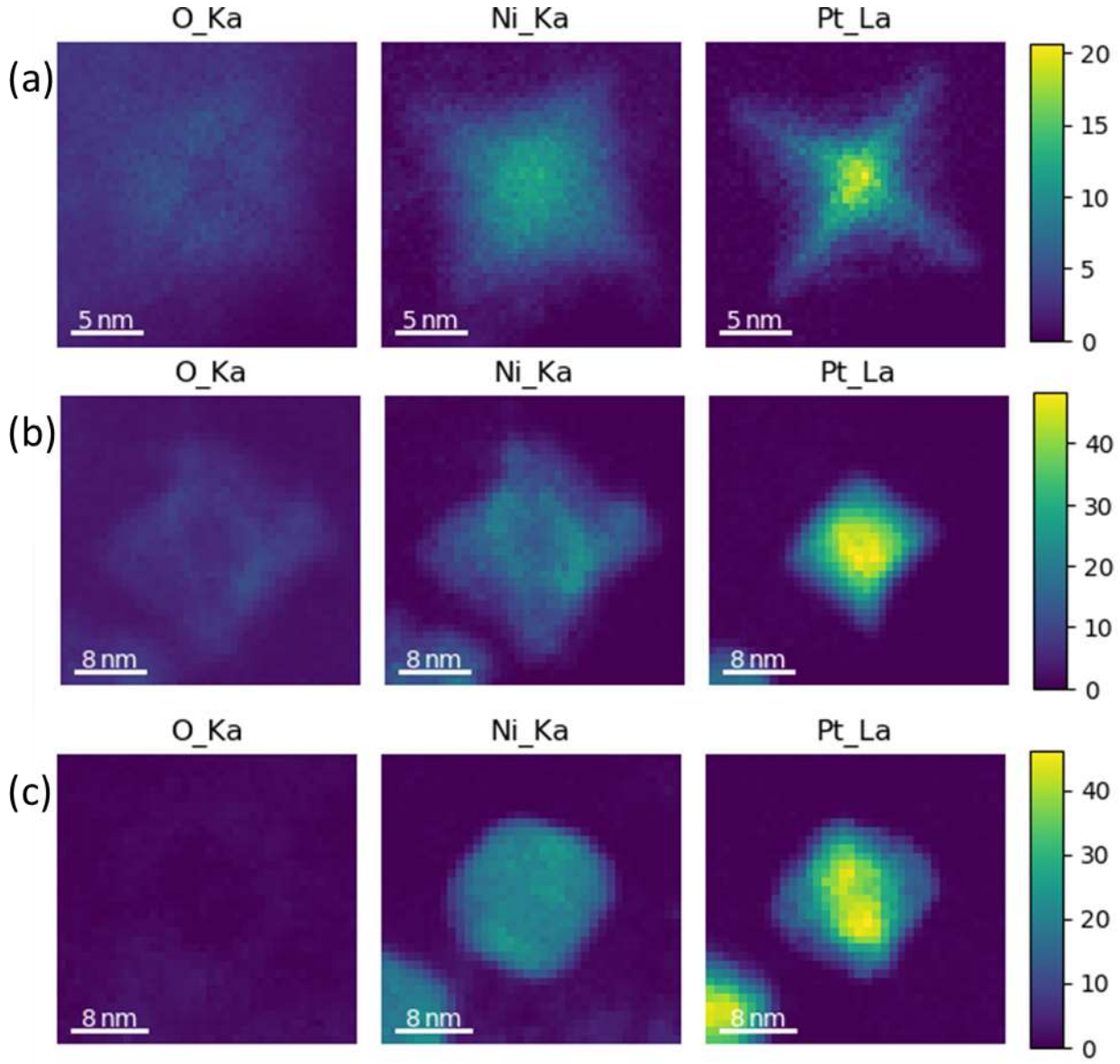

Figure S10. EDS Elemental maps, after NMF analysis for O Ka, Ni Ka and Pt La plotted on the same intensity scale for (a) oh-PtNi(Mo)-17, (b) oh-PtNi(Mo)-17A and (c) oh-PtNi(Mo)-17H structures viewed along the <100> direction. The intensity scale is in X-ray counts.

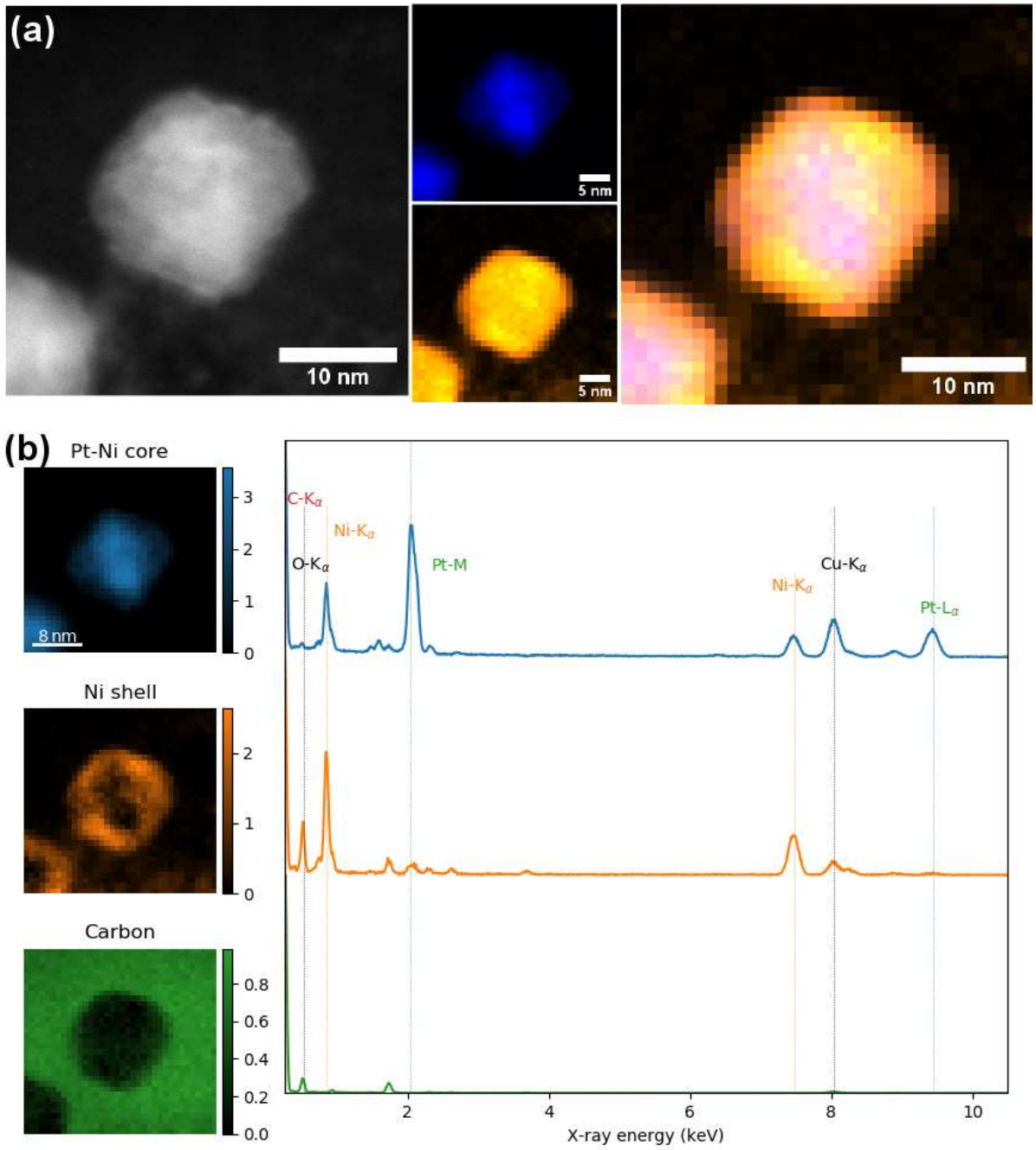

Figure S11. H_2-annealed oh-PtNi(Mo)-17H: (a) ADF-STEM micrograph and STEM-EDS elemental mapping for Pt (blue) and Ni (yellow), and their overlay, viewed a) along a <100> direction. (b) EDS NMF component maps and corresponding spectra show the distribution of a Pt-rich core (blue), a Ni- and O-rich shell (orange), as well as C (green).

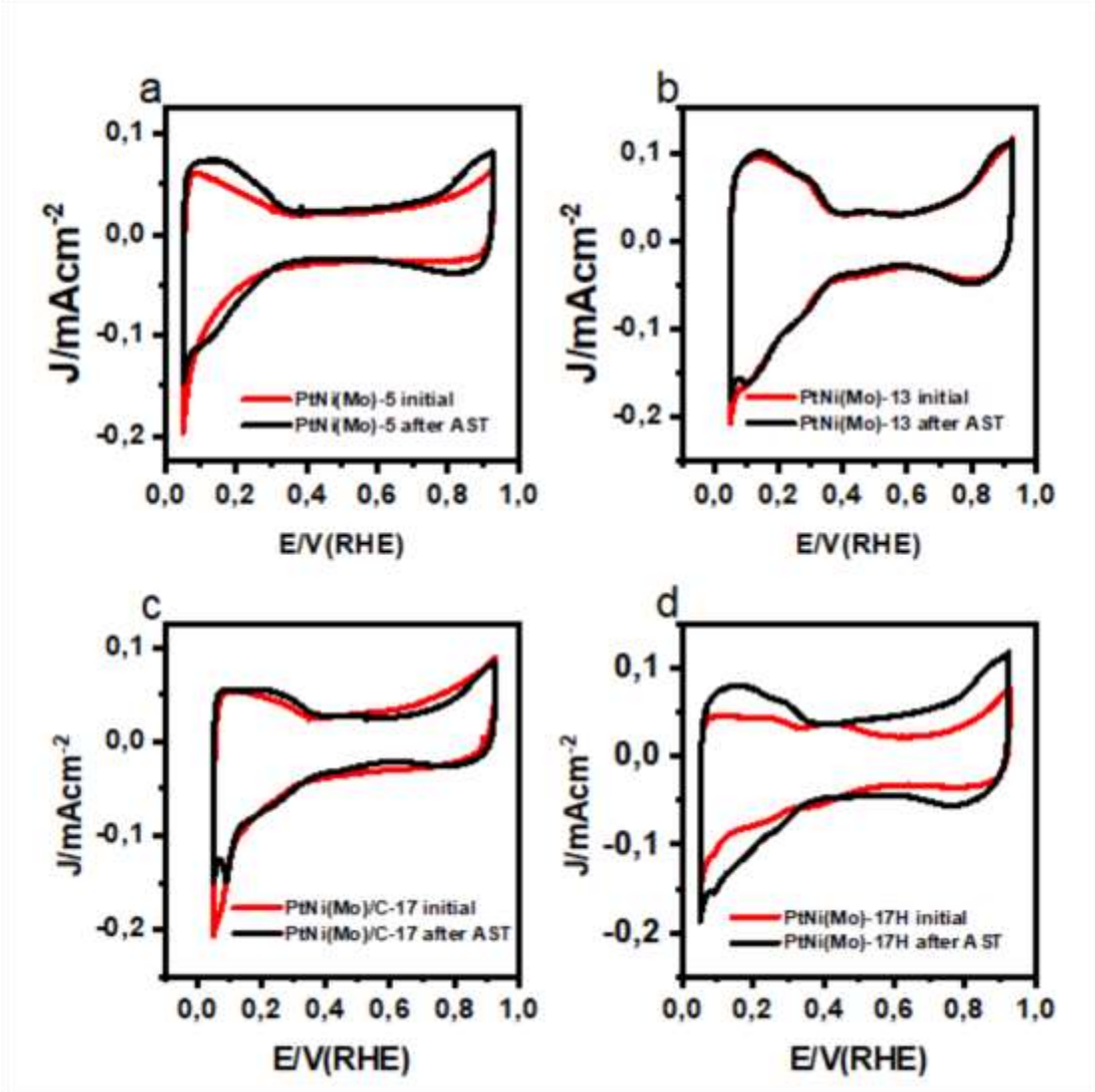

Figure S12. Electrochemical characterization of PtNi(Mo) series (iR corrected): cyclic voltammograms in N_2 saturated linear sweep voltammetry in 0.1M $HClO_4$ electrolyte before (red) and after (black) AST between 0.6–0.95 V_{RHE} for (a) PtNi(Mo)-5, (b) PtNi(Mo)-13, (c) PtNi(Mo)-17 and (d) PtNi(Mo)-17H.

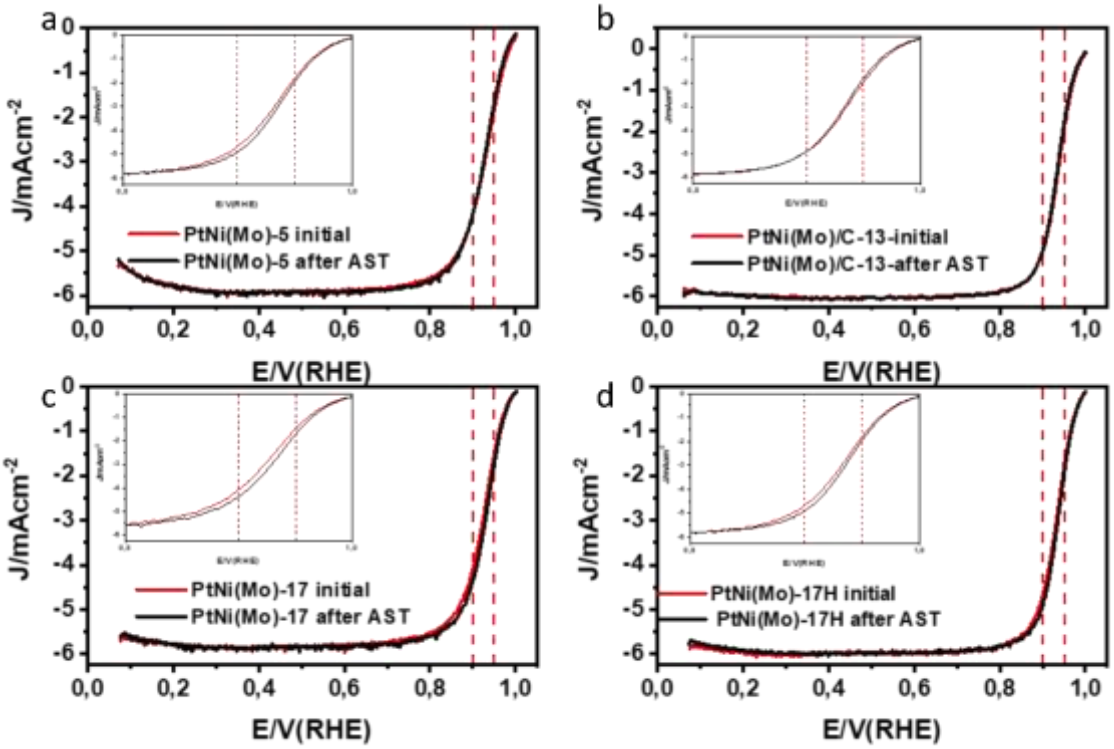

Figure S13. Electrochemical characterization of the PtNi(Mo) series (iR corrected): linear sweep voltammetry in 0.1M $HClO_4$ electrolyte before (red) and after (black) AST between 0.65–0.95 V_{RHE}. Insets show magnification for potentials around 0.9 and 0.95V_{RHE} where activities were sampled, for (a) PtNi(Mo)-5, (b) PtNi(Mo)-13, (c) PtNi(Mo)-17 and (d) PtNi(Mo)-17H.

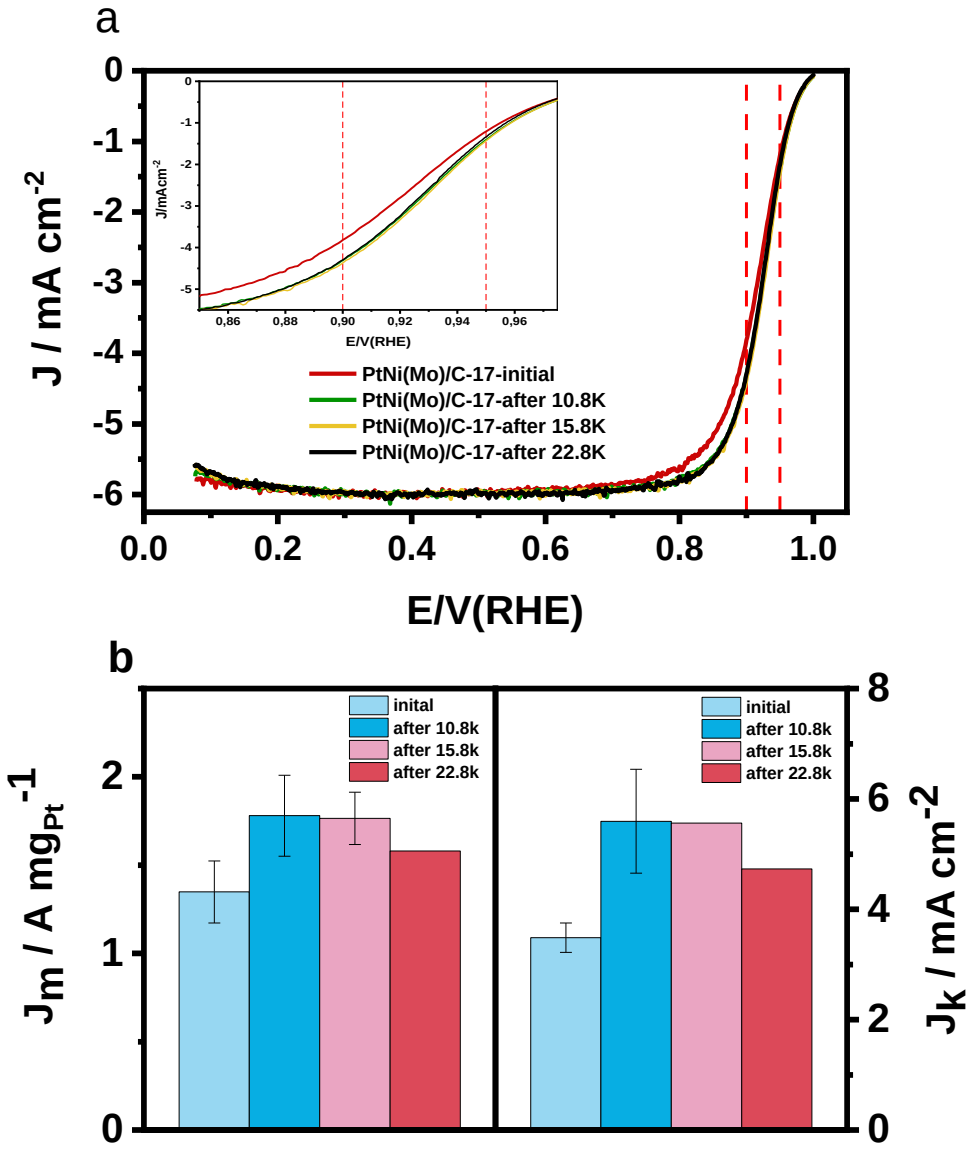

Figure S14. Electrochemical stability testing of PtNi(Mo)-17 (a) ORR polarization curves, inset shows magnification for potentials around 0.9 and 0.95V_{RHE} where activities were sampled (b) Mass activities (left) and specific activities (right).

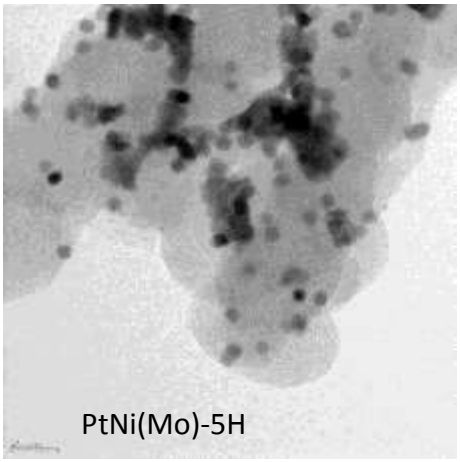

Figure S15. TEM images of (a) oh-PtNi(Mo)-5 after annealing in H_2 environment and (b) as-prepared bimetallic PtNi-13.

Table S2. Electrochemical performance and stability. $ECSA_{Hupd}$ and $ECSA_{CO}$ before and after ASTs, mass and specific activities before and after ASTs (evaluated at 0.9 and 0.95 V_{RHE})

Catalysts	Based on H_{upd} stripping				Based on CO stripping					
	ECSA (m^2/g_{Pt})		Specific activity @0.9 V (@0.95 V) (mA/cm^2)		ECSA (m^2/g_{Pt})		Specific activity @0.9 V (@0.95 V) (mA/cm^2)		Mass activity @0.9 V (@0.95 V) (A/mg_{Pt})	
	Before AST	After AST	Before AST	After AST	Before AST	After AST	Before AST	After AST	Before AST	After AST
PtNi(Mo)-5	43.0	48.4	4.96 (0.89)	4.29 (0.70)	52.3	52.1	4.13 (0.69)	3.98 (0.65)	2.13 (0.37)	2.08 (0.34)
PtNi(Mo)-13	45.3	46.8	5.08 (0.51)	4.80 (0.51)	48.3	46.9	5.14 (0.51)	5.52 (0.55)	2.42 (0.24)	2.26 (0.26)
PtNi(Mo)-17	35.0	36.3	3.76 (0.54)	5.56 (0.74)	39.9	33.8	3.56 (0.50)	5.60 (0.81)	1.40 (0.19)	2.17 (0.27)
PtNi(Mo)-17H	20.8	40.8	10.96 (1.25)	6.55 (0.69)	39.3	38.9	4.88 (0.56)	6.87 (0.73)	2.29 (0.26)	2.65 (0.28)
PtNi(Mo)-5H	26.8	24.1	0.24	0.86	25.0	26.2	0.29	0.79	0.065	0.21
PtNi-13	38.4	41.8	3.71	3.92	32.9	27.9	4.4	5.86	1.45	1.64

References.

(1) Rudi, S.; Cui, C.; Gan, L.; Strasser, P. Comparative Study of the Electrocatalytically Active Surface Areas (ECSAs) of Pt Alloy Nanoparticles Evaluated by Hupd and CO-Stripping Voltammetry. *Electrocatalysis* **2014**, *5* (4), 408–418. https://doi.org/10.1007/s12678-014-0205-2.